Fast, tissue-realistic models of photoacoustic wave propagation for homogeneous attenuating media

Bradley E. Treeby[*a], Benjamin T. Cox[a]
[a]Department of Medical Physics and Bioengineering, University College London, Gower Street, London, WC1E 6BT, United Kingdom

ABSTRACT

Photoacoustic tomography is an emerging medical imaging modality based on the reconstruction of an initial internal pressure distribution from surface measurements of photoacoustic wave pulses over time. Current methods used for this image reconstruction assume that the propagation medium is acoustically non-attenuating. However, in soft biological tissue, the frequency dependent ultrasonic attenuation is sufficient to cause considerable distortion to photoacoustic waves, even over short propagation distances. This distortion introduces blurring artifacts into images reconstructed under the assumption of a lossless medium. Here, a general lossy wave equation applicable to biological media is developed for which an exact solution (formed in the wavenumber-frequency domain) is derived. Explicit consideration is given to sound speed dispersion which is shown to have a negligible effect on photoacoustic imaging. Given an initial pressure distribution, the developed model allows the complete pressure field within the domain to be computed at an arbitrary time without iteration. The computation relies only on the Fourier transform and a decaying time propagator dependent on the attenuation in the medium. This facilitates the fast calculation of pressure fields in two or three dimensions over large domains. The model is demonstrated through the simulation and reconstruction of an example pulse distribution in a lossy medium.

Keywords: photoacoustic imaging, ultrasound propagation, ultrasound modeling, acoustic attenuation, dispersion, k-space models

1. INTRODUCTION

Photoacoustic tomography (PAT) is an emerging medical imaging modality that is particularly useful for the *in vivo* visualization of superficial vascular structures [1]. The technique exploits the photoacoustic effect in which the localized absorption of light (particularly by the hemoglobin chromophores present in blood) produces ultrasonic waves via thermo-elastic expansion. By measuring the ultrasonic waves that propagate to the skin surface, images of the absorbed optical energy distribution can be reconstructed. The particular algorithm used for this reconstruction is dependent on the geometry of the measurement system, but is typically based on the back projection or time reversal of a forward propagation model [2].

Currently, reconstruction models make the assumption that the propagation medium is acoustically non-attenuating. However, the acoustic attenuation in human fat is approximately $0.6\,dB\,MHz^{-1}\,cm^{-1}$ [3] and as much as $3\,dB\,MHz^{-1}\,cm^{-1}$ in the dermis layer of human skin [4]. In the context of PAT, the produced ultrasonic pulses are on the order of $10\,ns$ giving a broadband frequency content from the kilohertz range to many tens of megahertz. Consequently, the frequency dependent acoustic attenuation in biological media can cause considerable distortion to the shape of the propagating waves (the high frequency components are readily absorbed, even over small propagation distances). For photoacoustic image reconstruction, this distortion produces a blurring effect which limits the achievable resolution of the modality.

Recently, a method to correct for ultrasonic attenuation in photoacoustic simulations and reconstructions has been proposed [5]. This is based on an established time domain wave equation for media with attenuation following a general power law [6]. The correction term is formed as an integral equation dependent on a complex dispersive wavenumber and the ultrasonic pressure in the absence of attenuation. The method has been used to illustrate the considerable blurring artifacts introduced by attenuation in conventional image reconstruction [7]. Here, a k-space solution for wave propagation in a homogeneous attenuating medium is presented. First, the loss mechanisms responsible for acoustic

[*] btreeby@mpb.ucl.ac.uk; phone +44 (0) 20 7679 7086; http://www.medphys.ucl.ac.uk/research/mle

Photons Plus Ultrasound: Imaging and Sensing 2009: The Tenth Conference on Biomedical Thermoacoustics, Optoacoustics, and Acousto-optics, edited by Alexander A. Oraevsky, Lihong V. Wang, Proc. of SPIE Vol. 7177, 717716, (2009) · 1605-7422/09/$18 · doi: 10.1117/12.806794

attenuation are described. Next, a general frequency domain lossy wave equation applicable to biological media is developed with explicit consideration given to the effect of dispersion (frequency dependent sound speed) on photoacoustic imaging. An exact solution is then derived which, given a initial pressure distribution, allows the pressure field at an arbitrary time to be computed without iteration. The solution is formed in the wavenumber-frequency domain (k-space) and computationally is considerably more efficient than solutions based on Poisson's solution for an initial value problem or other methods that utilize finite differences to approximate derivatives [8]. Finally, the derived propagation model is demonstrated through a simulation and reconstruction example which illustrates the effect of acoustic attenuation in biological media on photoacoustic imaging.

2. FORMULATION OF A FREQUENCY DOMAIN LOSSY WAVE EQUATION

The transmission of a linear acoustic wave through a lossy fluid medium is accompanied by the diffusion of heat and momentum as well as energy exchanges on a molecular level [9, 10]. These absorption processes cause the gradual degradation of acoustic energy into thermal energy, and consequently, the attenuation of the wave amplitude. Heat diffusion (or thermal conduction) occurs because the small changes in excess pressure are not exactly adiabatic, nor isothermal (there is not time between pressure fluctuations for the temperature to stabilize) [9]. As a result, a small amount of heat energy irreversibly flows from higher temperature regions (pressure compressions where there is faster average molecular motion) to lower temperature regions (pressure rarefactions where there is slower average molecular motion). Momentum diffusion is caused by internal friction (viscosity) between adjacent regions of the propagation medium with differing motion. The shear viscosity characterizes the losses that accompany shear deformation, and the bulk (or volume) viscosity characterizes the stiffness force that resists compression. The latter is physically related to the time to establish thermodynamic equilibrium between translational and rotational molecular vibration.

The net result of these loss mechanisms is a lag in the oscillation of the medium density following a change in the excess pressure (physically, the change in pressure is responsible for fluid motion which in turn causes a change in density). Phenomenologically, this lag can be modeled by introducing a time delay (or relaxation time) into the adiabatic equation of state used in the derivation of the lossless wave equation (an approach first taken by Stokes). Similarly, the governing continuity equations can be explicitly modified to include viscosity and thermal conduction to yield the thermo-viscous wave equation [11].

Over the frequency spectrum used for medical ultrasound, the classical lossy wave equations predict an attenuation parameter that is dependent on frequency squared. However, the ultrasonic attenuation empirically observed in most soft biological tissue follows a frequency power law of the form

$$\alpha = \alpha_0 f^y \ , \tag{1}$$

where $y \approx 1$ [12] (the attenuation is typically given in units of $dB\,MHz^{-y}\,cm^{-1}$). The disparity between the observed attenuation and the classical wave equations is because, in addition to the thermal relaxation between translational and rotational degrees of molecular freedom (characterized by the bulk viscosity coefficient included in the thermo-viscous wave equation), there are also other chemical and molecular relaxation processes occurring that cause a gradual degradation of the acoustic energy [13].

Over a given frequency range, the power law attenuation observed in biological tissue can be modeled by fitting a complex compressibility coefficient which includes a number of relaxation parameters [14]. This approach has previously been incorporated into a k-space model for heterogeneous media [15]. However, to model power law attenuation over a wide frequency range (as required for photoacoustic tomography) several different relaxation parameters must be used. This increases the storage and mapping requirements for time stepping k-space solutions and makes other analytical solutions difficult to obtain [6].

A more apposite wave equation can be derived by considering a generalized dispersion relation that directly incorporates a power law attenuation term;

$$k = \frac{\omega}{c_p(\omega)} + i\hat{\alpha}_0 |\omega|^y \ . \tag{2}$$

Here k is the spatial wavenumber, ω is the angular frequency in $rad\,s^{-1}$, $c_p(\omega)$ is the dispersive sound speed in $m\,s^{-1}$, and $\hat{\alpha} = \hat{\alpha}_0 \omega^y$ is the attenuation in units of $Nepers\,(rad/s)^{-y}\,m^{-1}$. The conversion between $\hat{\alpha}_0$ and α_0 (in units of $dB\,MHz^{-y}\,cm^{-1}$) is achieved using the relation

$$\hat{\alpha}_0 = \frac{100\alpha_0}{8.686}\left(\frac{10^{-6}}{2\pi}\right)^y . \tag{3}$$

Returning to Eq. (2), the absolute value sign in the second term is required to satisfy the decaying physical condition in which waves travelling both forward and backward in space decay with time (the attenuation is a real and even function of frequency). Taking the square of this equation and multiplying by $P(\mathbf{k},\omega)$ yields a generalized frequency domain lossy wave equation

$$\left(k^2 - \frac{\omega^2}{c_p(\omega)^2} - 2i\frac{\omega}{c_p(\omega)}\hat{\alpha}_0|\omega|^y + \hat{\alpha}_0{}^2|\omega|^{2y}\right)P(\mathbf{k},\omega) = 0 . \tag{4}$$

Here $P(\mathbf{k},\omega)$ is the four-dimensional (4D) Fourier transform of the excess pressure $p(\mathbf{r},t)$ (using the Fourier transform conventions defined in Ref. [9]), and $\mathbf{k} = \{k_x, k_y, k_z\}$. For $y = 1$, this reduces to a frequency domain lossy wave equation suitable for modeling linear ultrasound propagation in homogeneous soft biological tissue

$$\left(k^2 - \frac{\omega^2}{c_p(\omega)^2} - \mathrm{sgn}(\omega)2i\hat{\alpha}_0\frac{\omega^2}{c_p(\omega)}\right)P(\mathbf{k},\omega) = 0 . \tag{5}$$

Here sgn is the signum function (note, for $y = 1$ the final term in Eq. (4) can be neglected as $\hat{\alpha}_0{}^2 c_p(\omega)^2 << 1$). Under the conditions of stress confinement (in which the absorbed optical energy can be approximated by $H(\mathbf{r},t) \approx h(\mathbf{r})\delta(t)$), a photoacoustic source term can be added to this expression as a time domain initial condition $p(\mathbf{r},0) = \Gamma h(\mathbf{r})$ [16]. Here Γ is the non-dimensional Grüneisen parameter which characterizes the efficiency of the conversion of absorbed optical energy $h(\mathbf{r})$ into pressure.

To satisfy absolute causality (in which an effect cannot precede its cause), the attenuation $\hat{\alpha}_0|\omega|^y$ and dispersive sound speed $c_p(\omega)$ in the governing dispersion relation must be related via the Kramers-Krönig integral equations. For wave propagation in media with attenuation following a frequency power law where $0 < y < 3$, the appropriate Kramers-Krönig relation is given by [17]

$$c_p(\omega) = \left[\frac{1}{c_0} + \hat{\alpha}_0 \tan\left(\frac{y\pi}{2}\right)\left(\omega^{y-1} - \omega_0{}^{y-1}\right)\right]^{-1} . \tag{6}$$

Here the dispersion is given as a variation from a reference sound speed $c_P(\omega_0) = c_0$ at a particular frequency ω_0. For $y = 1$ this reduces to

$$c_p(\omega) = \left[\frac{1}{c_0} - \frac{2}{\pi}\hat{\alpha}_0 \ln\left(\frac{\omega}{\omega_0}\right)\right]^{-1} . \tag{7}$$

A non-dispersive version of Eq. (4) (again omitting the final term) was similarly considered by Szabo in the derivation of a time domain lossy wave equation [18, 19].[1] Other approaches to develop time domain expressions for Eq. (4) have also been proposed, where the equations provided by Sushilov & Cobbold (following Szabo) were used in the derivation of the attenuation correction method described in the introduction [6]. Here, a solution in the wavenumber-frequency domain is developed.

[1] In his derivation, Szabo first considered a non-causal time domain wave equation which he then modified by adding an extra term to the real part of the complex wavenumber related to the power law attenuation through the Hilbert transform. The final form of Szabo's time domain wave equation also satisfies the Kramers-Krönig relations given in Eqs. (6) and (7) as required by causality.

3. QUANTIFYING THE EFFECT OF DISPERSION ON PHOTOACOUSTIC IMAGING

The consequence of a dispersive sound speed on wave propagation is a gradual change in the wave shape with propagation distance. However, for photoacoustic tomography *in vivo*, the propagation distance is restricted by ultrasonic attenuation, scattering and absorption of the excitation laser source, and safe limits of laser exposure. This typically confines the imaging region to depths of less than $20\,mm$. To examine the effect of dispersion on photoacoustic imaging, it is constructive to consider the propagation of a plane wave pulse through an attenuating and dispersive medium (see Fig. 1). After some time t, the complete wave pulse will travel a distance $z_0 = c_0 t$, where c_0 is the nominal sound speed (i.e., the group velocity). If the propagating wave pulse is composed of a series of monochromatic waves travelling from an identical spatial location for the same length of time, the dispersive sound speed (i.e., the frequency dependent phase speed) will result in a frequency dependent propagation distance $z(\omega)$, where $z(\omega) = c_p(\omega)t$. The distance disparity between $z(\omega)$ and z_0 will 'blur' the shape of the original wave pulse where $\Delta z = z(\omega) - z_0 = \Delta c\, t$. If the pulse is detected at a particular point and the propagation medium is assumed to be non-dispersive, the blurred (or dispersive) wave pulse will then be reconstructed at the location of the original wave pulse.

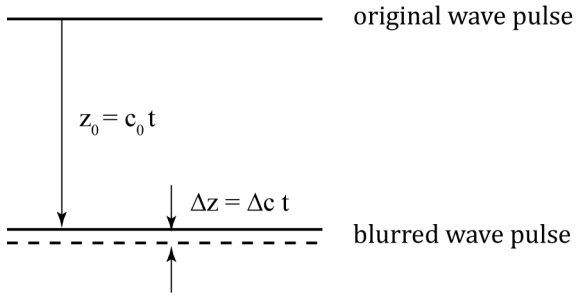

Fig. 1. Blur of a plane wave pulse in a dispersive propagation medium.

Given a characteristic spatial resolution d, it is legitimate to neglect dispersion provided that $\Delta z < d$, i.e., the dispersion blur is smaller than the corresponding spatial resolution of the detection system. For $y = 1$, $c_p(\omega)$ can be calculated using Eq. (7) giving

$$\Delta c = c_p(\omega) - c_0 = \frac{2c_0^{\,2}\hat{\alpha}_0 \ln\left(\frac{\omega}{\omega_0}\right)}{\pi - 2c_0\hat{\alpha}_0 \ln\left(\frac{\omega}{\omega_0}\right)} \approx \frac{2}{\pi} c_0^{\,2}\hat{\alpha}_0 \ln\left(\frac{\omega}{\omega_0}\right). \tag{8}$$

Combining this with the inequality $\Delta z < d$ yields

$$\frac{2}{\pi} \ln\left(\frac{\omega}{\omega_0}\right) z_0 \hat{\alpha}_0 c_0 < d\,, \tag{9}$$

where the left term (Δz) is the dispersion blur. This is plotted in Fig. 2(a) as a function of frequency and propagation distance using a reference frequency of $\omega_0 = 2\pi \times 10^6\ rad\,s^{-1}$ ($1\,MHz$) and the acoustic properties of human fat, where $\hat{\alpha}_0 = 1.1 \times 10^{-6}\ Nepers\,rad^{-1}\,s\,m^{-1}$ ($\alpha_0 = 0.6\ dB\,MHz^{-1}\,cm^{-1}$) and $c = 1430\,m\,s^{-1}$ [3]. Over the complete depth and frequency range considered, the dispersion blur remains below $70\,\mu m$. It is a maximum for wideband sources and large propagation depths. For depths less than $10\,mm$ it remains below $40\,\mu m$, and for depths less than $5\,mm$ below $20\,\mu m$.

By comparison, at an imaging depth of $5\,mm$ the *lateral* resolution of current optical ultrasound detection systems useful for photoacoustic imaging is approximately $70\,\mu m$ [20]. This decreases as the imaging depth is increased. Although the spatially invariant *depth* resolution can be significantly higher (on the order of $20\,\mu m$ for a $22\,\mu m$ sensor), for planar measurements the lateral resolution ultimately limits the effective resolution [20]. For a given imaging depth, the minimum achievable lateral resolution is also limited by the physical focus size of the sensor laser beam as well as the

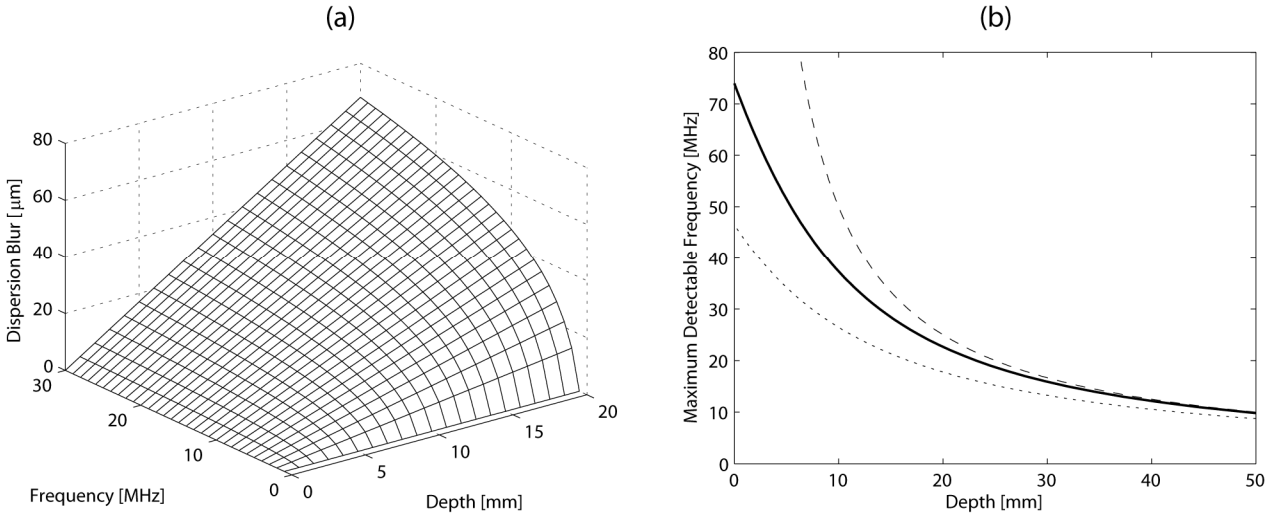

Fig. 2. (a) Dispersion blur as a function of frequency and propagation depth for an attenuation value of $\alpha_0 = 0.6$. (b) The maximum detectable frequency with propagation depth for an attenuation value of $\alpha_0 = 0.6$ and a dynamic range of $30\,dB$, given; a delta function pulse (upper curve), an $8\,ns$ Gaussian wave pulse (middle curve), and an $8\,ns$ Gaussian wave pulse including an additional $1.5\,mm$ layer of skin with an attenuation value of $\alpha_0 = 2.6$ (lower curve).

scanning step angle. It is important to note that, for *in vivo* imaging, sound speed and density heterogeneities, approximated acoustic properties, finite sensor apertures, and subject motion will all introduce artifacts into the reconstructed image which will additionally reduce the effective resolution.

In addition to sensor resolution, it is also constructive to consider the effect of attenuation on the detectable frequency bandwidth, as this will also restrict the dispersion blur. The peak photoacoustic pressures generated *in vivo* are typically $5-10\,kPa$ while a high sensitivity Fabry-Perot sensor has noise equivalent pressure of $\sim 0.2\,kPa$ giving a dynamic range on the order of $30\,dB$ [20]. Again using an attenuation value of $\alpha_0 = 0.6\,dB\,MHz^{-1}\,cm^{-1}$ (fat), the maximum detectable frequency as a function of imaging depth is shown in Fig. 2(b). The upper curve (dashed line) is for a delta function pulse, the middle curve (solid line) is for an $8\,ns$ Gaussian wave pulse, and the lower curve (dotted line) is for an $8\,ns$ Gaussian wave pulse including an additional $1.5\,mm$ skin layer with an attenuation value of $\alpha_0 = 2.6\,dB\,MHz^{-1}\,cm^{-1}$ (human dermis for the $15-30$ year age group [4]). For an imaging depth of $20\,mm$, the maximum detectable frequency for a Gaussian wave pulse is restricted to $23\,MHz$ ($25\,MHz$ and $18\,MHz$ respectively for the delta pulse and the Gaussian pulse with skin). Examination of Fig. 2(a) illustrates that this bandwidth restriction will further limit the detectable effects of dispersion. In light of the preceding discussion, it can be concluded that for PAT, the effects of dispersion can legitimately be neglected.

4. MODELING WAVE PROPAGATION IN K-SPACE

For an infinite domain initial value problem of the form $\mathrm{L}p(\mathbf{r},t) = 0$ (where L is a general linear operator), a general solution can be formed using Green's second identity [21], where

$$p(\mathbf{r},t) = \frac{1}{c^2}\int\left[g(\mathbf{r},t \mid \mathbf{r}_0,t_0)\frac{\partial p(\mathbf{r}_0,t_0)}{\partial t_0} - p(\mathbf{r}_0,t_0)\frac{\partial g(\mathbf{r},t \mid \mathbf{r}_0,t_0)}{\partial t_0}\right] d\mathbf{r}_0 \,. \tag{10}$$

Here the Green's function $g(\mathbf{r},t \mid \mathbf{r}_0,t_0)$ is a solution to the equation $\mathrm{L}g(\mathbf{r},t \mid \mathbf{r}_0,t_0) = -\delta(\mathbf{r}-\mathbf{r}_0)\delta(t-t_0)$. Given initial conditions $t_0 = 0$, $p(\mathbf{r},0) = p_0(\mathbf{r})$, and $\partial p(\mathbf{r},0)/\partial t = 0$, Eq. (10) becomes

$$p(\mathbf{r},t) = \frac{1}{c^2}\int p_0(\mathbf{r}_0)\frac{\partial g(\mathbf{r},t \mid \mathbf{r}_0,t_0)}{\partial t} d\mathbf{r}_0 \,, \tag{11}$$

(where $dg/dt_0 = -dg/dt$). Neglecting dispersion (i.e., setting $c_p(\omega) = c$), the frequency domain lossy wave equation developed in Section 2 may be written as

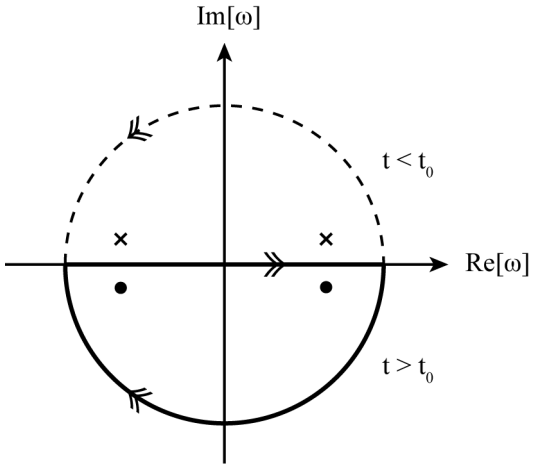

Fig. 3. Contour integration and pole location for the singular integrand given in Eq. (17).

$$\left(\frac{\omega^2}{c^2}+\mathrm{sgn}\left(\omega\right)2i\hat{\alpha}_0\frac{\omega^2}{c}-k^2\right)P\left(\mathbf{k},\omega\right)=0\,, \tag{12}$$

where the corresponding Green's function represents a solution to

$$\left(\frac{\omega^2}{c^2}+\mathrm{sgn}\left(\omega\right)2i\hat{\alpha}_0\frac{\omega^2}{c}-k^2\right)G\left(\mathbf{k},\omega\right)=-\frac{1}{\left(2\pi\right)^4}e^{i\omega t_0}e^{-i\mathbf{k}\cdot\mathbf{r}_0}\,. \tag{13}$$

Solving for $G\left(\mathbf{k},\omega\right)$ and taking the inverse 4D Fourier transform then yields the required time domain Green's function

$$g\left(\mathbf{r},t\,|\,\mathbf{r}_0,t_0\right)=-\frac{c^2}{\left(2\pi\right)^4}\iint\frac{e^{-i\omega\left(t-t_0\right)}e^{i\mathbf{k}\cdot\left(\mathbf{r}-\mathbf{r}_0\right)}}{\omega^2+\mathrm{sgn}\left(\omega\right)2i\hat{\alpha}_0c\omega^2-c^2k^2}d\omega d\mathbf{k}\,. \tag{14}$$

This expression is not yet computationally useful due to the singularities in the integrand; depending on $\mathrm{sgn}\left(\omega\right)$ there are two sets of simple poles, where

$$\omega=\pm\frac{ck}{\sqrt{1+2i\hat{\alpha}_0c}},\pm\frac{ck}{\sqrt{1-2i\hat{\alpha}_0c}}\,. \tag{15}$$

To remove the singularities, the integration with respect to ω can be evaluated analytically using contour integration. The contour is taken along the real axis and returned by a semi-circle of infinite radius. For $t>t_0$, the contour is completed below the real axis (because of the negative exponential exponent) and for $t<t_0$ it is completed above (see Fig. 3). For $t>t_0$, there are two poles contained within the contour, where

$$\omega_{p1,p2}=\frac{ck}{\sqrt{1+2i\hat{\alpha}_0c}},\frac{-ck}{\sqrt{1-2i\hat{\alpha}_0c}}\,. \tag{16}$$

For $t_0=0$, the integral solution is then formed using the sum of residuals for a clockwise contour

$$\int_\omega=\int\frac{e^{-i\omega t}}{\omega^2+\mathrm{sgn}\left(\omega\right)2i\hat{\alpha}_0c\omega^2-c^2k^2}d\omega=-2\pi i\left[R\left(\omega_{p1}\right)+R\left(\omega_{p2}\right)\right], \tag{17}$$

where $R\left(\omega_p\right)$ is the residual at ω_p given by $R\left(\omega_p\right)=\lim_{\omega\to\omega_p}\left(\omega-\omega_p\right)F\left(\omega_p\right)$. The required residuals are given by

$$R(\omega_{p1}) = \lim_{\omega \to \omega_{p+}} (\omega - \omega_{p1}) \frac{e^{-i\omega t}}{\omega^2 + 2i\hat{\alpha}_0 c\omega^2 - c^2 k^2} = \frac{e^{\frac{-ickt}{\sqrt{1+2i\hat{\alpha}_0 c}}}}{2ck\sqrt{1+2i\hat{\alpha}_0 c}}$$
$$R(\omega_{p2}) = \lim_{\omega \to \omega_{p+}} (\omega - \omega_{p2}) \frac{e^{-i\omega t}}{\omega^2 - 2i\hat{\alpha}_0 c\omega^2 - c^2 k^2} = -\frac{e^{\frac{ickt}{\sqrt{1-2i\hat{\alpha}_0 c}}}}{2ck\sqrt{1-2i\hat{\alpha}_0 c}} \quad . \tag{18}$$

Combining Eqs. (17) and (18), the Green's function given in Eq. (14) can now be written as

$$g(\mathbf{r}, t \mid \mathbf{r}_0, t_0) = \frac{c^2}{(2\pi)^3} \int \left[\frac{1}{2} \frac{ie^{\frac{-ickt}{\sqrt{1+2i\hat{\alpha}_0 c}}}}{ck\sqrt{1+2i\hat{\alpha}_0 c}} - \frac{1}{2} \frac{ie^{\frac{ickt}{\sqrt{1-2i\hat{\alpha}_0 c}}}}{ck\sqrt{1-2i\hat{\alpha}_0 c}} \right] e^{i\mathbf{k}\cdot(\mathbf{r}-\mathbf{r}_0)} d\mathbf{k} \,, \tag{19}$$

where the corresponding temporal derivative is

$$\frac{\partial g(\mathbf{r}, t \mid \mathbf{r}_0, t_0)}{\partial t} = \frac{c^2}{(2\pi)^3} \int \left[\frac{1}{2} \frac{e^{\frac{-ickt}{\sqrt{1+2i\hat{\alpha}_0 c}}}}{1+2i\hat{\alpha}_0 c} + \frac{1}{2} \frac{e^{\frac{ickt}{\sqrt{1-2i\hat{\alpha}_0 c}}}}{1-2i\hat{\alpha}_0 c} \right] e^{i\mathbf{k}\cdot(\mathbf{r}-\mathbf{r}_0)} d\mathbf{k} \,. \tag{20}$$

This finally gives Eq. (11) (for $t > 0$) as

$$p(\mathbf{r}, t) = \frac{1}{(2\pi)^3} \iint p_0(\mathbf{r}_0) \left[\frac{1}{2} \frac{e^{\frac{-ickt}{\sqrt{1+2i\hat{\alpha}_0 c}}}}{1+2i\hat{\alpha}_0 c} + \frac{1}{2} \frac{e^{\frac{ickt}{\sqrt{1-2i\hat{\alpha}_0 c}}}}{1-2i\hat{\alpha}_0 c} \right] e^{i\mathbf{k}\cdot(\mathbf{r}-\mathbf{r}_0)} d\mathbf{k} d\mathbf{r}_0 \,. \tag{21}$$

The integrals may be computed sequentially

$$p(\mathbf{r}, t) = \frac{1}{(2\pi)^3} \int \left[\int p_0(\mathbf{r}_0) e^{-i\mathbf{k}\cdot\mathbf{r}_0} d\mathbf{r}_0 \right] \left[\frac{1}{2} \frac{e^{\frac{-ickt}{\sqrt{1+2i\hat{\alpha}_0 c}}}}{1+2i\hat{\alpha}_0 c} + \frac{1}{2} \frac{e^{\frac{ickt}{\sqrt{1-2i\hat{\alpha}_0 c}}}}{1-2i\hat{\alpha}_0 c} \right] e^{i\mathbf{k}\cdot\mathbf{r}} d\mathbf{k} \,, \tag{22}$$

which in computational form is simply

$$p(\mathbf{r}, t) = \mathbb{F}_r^{-1} \left\{ \mathbb{F}_r \left\{ p_0(\mathbf{r}_0) \right\} TP \right\} , \tag{23}$$

where $\mathbb{F}$ is the fast Fourier transform, and the lossy time propagator TP is given by

$$TP = \frac{1}{2} \frac{e^{\frac{-ickt}{\sqrt{1+2i\hat{\alpha}_0 c}}}}{1+2i\hat{\alpha}_0 c} + \frac{1}{2} \frac{e^{\frac{ickt}{\sqrt{1-2i\hat{\alpha}_0 c}}}}{1-2i\hat{\alpha}_0 c} \,. \tag{24}$$

Equations (23) and (24) allow the pressure field in a homogeneous attenuating medium to be computed directly for an arbitrary propagation time and initial pressure distribution. For $\alpha_0 = 0$, Eq. (24) reduces to $TP = \cos(ckt)$ which is the conventional form of the lossless k-space time propagator [16, 22]. The decay of the lossy time propagator with time for $f = 10\,MHz$, $\alpha_0 = 0.6\,dB\,MHz^{-1}\,cm^{-1}$, and $c = 1430\,m \cdot s^{-1}$ (against the lossless time propagator) is shown in Fig. 4.

5. PHOTOACOUSTIC SIMULATION AND RECONSTRUCTION IN ATTENUATING MEDIA

The model developed in the previous section can be used to simulate the propagation of arbitrary wave pulses through attenuating media. To implement the model computationally, the initial pressure distribution must first be defined over a spatial grid in two or three dimensions, where N_x, N_y, and N_z define the number of grid points in the x, y, and z directions (and consequently the FFT length), and d_x, d_y, and d_z define the grid spacing. For example, if the initial

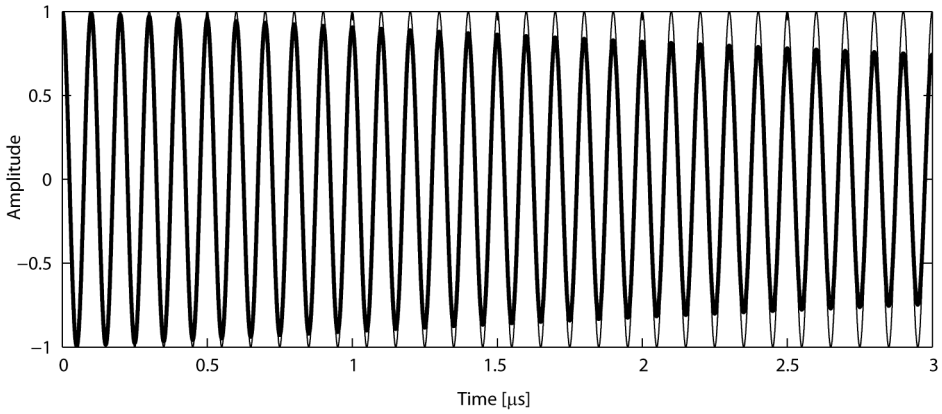

Fig. 4. Variation of the lossy (bold) and lossless (light) time propagators with time for $f = 10\,MHz$, $\alpha_0 = 0.6$, and $c = 1430\,m\,s^{-1}$.

pressure distribution $p_0(\mathbf{r}_0)$ is given by a two-dimensional image, then N_x and N_z would be the number of pixels in the x and z directions, and d_x and d_z would be the corresponding pixel widths. The matrix of wavenumbers is computed via the relation $k^2 = k_x^2 + k_y^2 + k_z^2$, where the k-space wavenumber components are given by evenly spaced vectors (duplicated across the other dimensions) on $-\pi / d_x \le k_x < \pi / d_x$ with N_x points (similarly for k_y and k_z). A simple two-dimensional example of a k-space simulation for the lossless time propagator (coded in Matlab®) is given in Ref [23].

To demonstrate the effect of acoustic attenuation on photoacoustic image reconstruction in biological media, the absorbing propagation model was used to simulate the pressure field generated by a two-dimensional pressure distribution as shown in Fig. 5(a). The time series from $0 - 6\,\mu s$ in steps of $2\,ns$ was computed at an array of receivers located on the border of a grid of 256×256 *pixels* (5.12×5.12 *mm* where $d_x = d_z = 20\,\mu m$)[2] with the attenuation in the medium set to $\alpha_0 = 3\,dB\,MHz^{-1}\,cm^{-1}$. Note that in the context of this example, the same total attenuation could be achieved by setting $\alpha_0 = 0.6\,dB\,MHz^{-1}\,cm^{-1}$ and recording the pressure over the border of a $25.6 \times 25.6\,mm$ grid (where the waves would travel on the order of $12\,mm$ before being detected). The time series recorded over the lower edge of the receiver grid is shown in Fig. 5(b). The time series recorded over all four grid edges was used to reconstruct the initial pressure distribution using a conventional time reversal algorithm assuming a non-attenuating medium [24]. The reconstructed pressure distribution is shown in Fig. 5(c). The slight diagonal banding artifacts are due to the finite length of the recorded time pulses; the reconstruction algorithm assumes the pressure within the domain before time reversal is exactly zero. In two-dimensions this requires infinitely long time pulses. Comparison of Fig. 5(a) and Fig. 5(c) illustrates that the attenuation has noticeably blurred the sharp edges of the original source function. This is also evident in Fig. 5(d) which shows an image slice through $z = 0$. A reduction in the magnitude of the pressure peaks is also clearly noticeable.

6. CONCLUSION

For photoacoustic imaging, the magnitude of acoustic attenuation in soft biological tissue is sufficient to cause perceptible blurring artifacts in images reconstructed assuming a lossless medium. For quantitative imaging, such as photoacoustic spectroscopy, these depth dependent magnitude errors will incorrectly influence the extraction of parameter values (for example, the hemoglobin content within a blood vessel [25]). Currently, there are very few methods available for efficiently modeling the propagation of photoacoustic waves in attenuating media. Here, an efficient technique for modeling wave propagation in tissue realistic media has been developed. The computation method relies only on the Fourier transform and a decaying time propagator dependent on the attenuation in the medium. This allows the fast calculation of pressure fields in two or three dimensions over large domains and also inherently facilitates parallelization. The solution may be particularly useful for studies attempting to quantify the effects of attenuation on image reconstruction algorithms. It is hoped that the method may be extended in the future to allow an analogous one-step back projection algorithm for an attenuating medium to be derived.

[2] The total grid size used for the forward simulation was actually 800×800 *pixels* to prevent wrap around effects due to the finite size of the propagation domain [16].

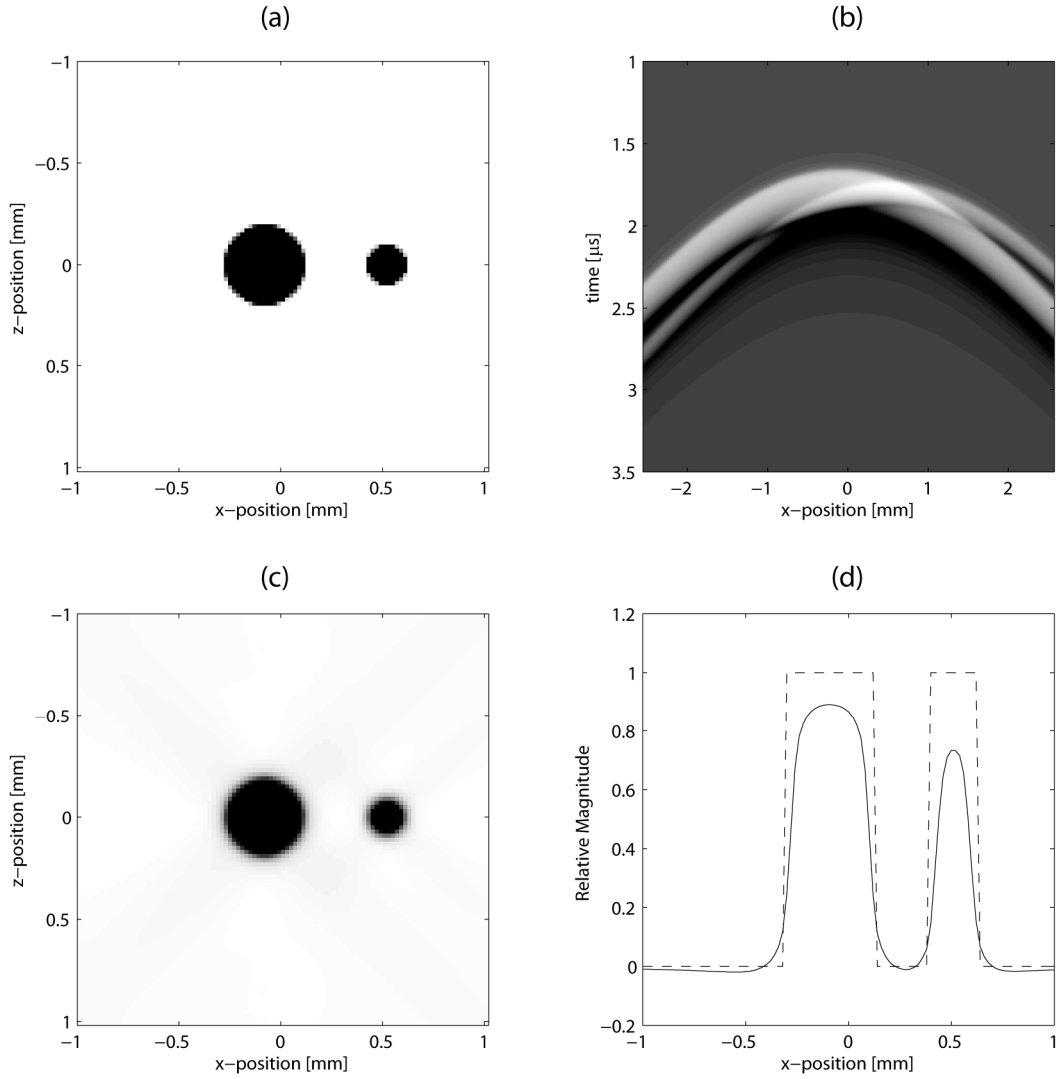

Fig. 5. Example of using a lossless reconstruction algorithm for photoacoustic tomography in biological media. (a) Assumed two-dimensional initial pressure distribution. (b) Time series data recorded over the lower edge of a 5.12×5.12 *mm* measurement grid. (c) Reconstructed image using a time reversal algorithm assuming a lossless medium. (d) Image slice through $z = 0$ where the dotted line shows the initial pressure distribution and the solid line the reconstructed pressure distribution.

ACKNOWLEDGMENTS

This work was supported by the Engineering and Physical Sciences Research Council, UK.

REFERENCES

[1] Zhang, E. Z., Laufer, J. G. and Beard, P. C., "Three dimensional photoacoustic imaging of vascular anatomy in small animals using an optical detection system," in *Proceedings of SPIE* 6437, 64370S-1 (2007).

[2] Kuchment, P. and Kunyansky, L., "Mathematics of thermoacoustic tomography," *Eur. J. Appl. Math.,* 19(2), 191-224 (2008).

[3] Szabo, T. L., [Diagnostic Ultrasound Imaging], Elsevier Academic Press, London (2004).

[4] Guittet, C., Ossant, F., Vaillant, L. and Berson, M., "In vivo high-frequency ultrasonic characterization of human dermis," *IEEE Trans. Biomed. Eng.,* 46(6), 740-746 (1999).
[5] La Rivière, P. J., Zhang, J. and Anastasio, M. A., "Image reconstruction in optoacoustic tomography for dispersive acoustic media," *Opt. Lett.,* 31(6), 781-783 (2006).
[6] Sushilov, N. V. and Cobbold, R. S. C., "Frequency-domain wave equation and its time-domain solutions in attenuating media," *J. Acoust. Soc. Am.,* 115(4), 1431-1436 (2004).
[7] La Rivière, P. J., Zhang, J. and Anastasio, M. A., "Ultrasonic attenuation correction in optoacoustic tomography," in *Proceedings of SPIE* 6086, 60861l-1 (2006).
[8] Cox, B. T., Kara, S., Arridge, S. R. and Beard, P. C., "k-space propagation models for acoustically heterogeneous media: Application to biomedical photoacoustics," *J. Acoust. Soc. Am.,* 121(6), 3453-3464 (2007).
[9] Morse, P. M. and Ingard, K. U., [Theoretical Acoustics], Princeton University Press, Princeton (1968).
[10] Kinsler, L. E., Frey, A. R., Coppens, A. B. and Sanders, J. V., [Fundamentals of Acoustics], Fourth ed., John Wiley & Sons, New York (2000).
[11] Markham, J. J., Beyer, R. T. and Lindsay, R. B., "Absorption of Sound in Fluids," *Rev. Mod. Phys.,* 23(4), 353-411 (1951).
[12] Duck, F. A., [Physical Properties of Tissue: A Comprehensive Reference Book], Academic Press, London (1990).
[13] Bhatia, A. B., [Ultrasonic Absorption], Oxford University Press, Oxford (1967).
[14] Nachman, A. I., Smith III, J. F. and Waag, R. C., "An equation for acoustic propagation in inhomogeneous media with relaxation losses," *J. Acoust. Soc. Am.,* 88(3), 1584-1595 (1990).
[15] Tabei, M., Mast, T. D. and Waag, R. C., "A k-space method for coupled first-order acoustic propagation equations," *J. Acoust. Soc. Am.,* 111(1), 53-63 (2002).
[16] Cox, B. T. and Beard, P. C., "Fast calculation of pulsed photoacoustic fields in fluids using k-space methods," *J. Acoust. Soc. Am.,* 177(6), 3616-3627 (2005).
[17] Waters, K. R., Hughes, M. S., Mobley, J., Brandenburger, G. H. and Miller, J. G., "On the applicability of Kramers-Krönig relations for ultrasonic attenuation obeying a frequency power law," *J. Acoust. Soc. Am.,* 108(2), 556-563 (2000).
[18] Szabo, T. L., "Time domain wave equations for lossy media obeying a frequency power law," *J. Acoust. Soc. Am.,* 96(1), 491-500 (1994).
[19] Szabo, T. L., "Causal theories and data for acoustic attenuation obeying a frequency power law," *J. Acoust. Soc. Am.,* 97(1), 14-24 (1995).
[20] Zhang, E., Laufer, J. G. and Beard, P. C., "Backward-mode multiwavelength photoacoustic scanner using a planar Fabry-Perot polymer film ultrasound sensor for high-resolution three-dimensional imaging of biological tissues," *Appl. Optics,* 47(4), 561-577 (2008).
[21] Jackson, J. D., [Classical Electrodynamics] vol. 9, Wiley, New York (1975).
[22] Köstli, K. P., Frenz, M., Bebie, H. and Weber, H. P., "Temporal backward projection of optoacoustic pressure transients using Fourier transform methods," *Phys. Med. Biol.,* 46(7), 1863-1872 (2001).
[23] Cox, B. T. and Beard, P. C., "Modeling Photoacoustic Propagation in Tissue Using k-Space Techniques," in [Photoacoustic Imaging and Spectroscopy], L. V. Wang, Ed., CRC Press (In Press).
[24] Burgholzer, P., Matt, G. J., Haltmeier, M. and Paltauf, G., "Exact and approximative imaging methods for photoacoustic tomography using an arbitrary detection surface," *Phys. Rev. E,* 75(4), 046706 (2007).
[25] Laufer, J. G., Delpy, D., Elwell, C. and Beard, P. C., "Quantitative spatially resolved measurement of tissue chromophore concentrations using photoacoustic spectroscopy: application to the measurement of blood oxygenation and haemoglobin concentration," *Phys. Med. Biol.,* 52(1), 141-168 (2007).